

See discussions, stats, and author profiles for this publication at: <https://www.researchgate.net/publication/40448216>

HIV-1 Protease Inhibitors with a Transition-State Mimic Comprising a Tertiary Alcohol: Improved Antiviral Activity in Cells

ARTICLE in JOURNAL OF MEDICINAL CHEMISTRY · DECEMBER 2009

Impact Factor: 5.45 · DOI: 10.1021/jm901165g · Source: PubMed

CITATIONS

25

READS

16

10 AUTHORS, INCLUDING:



Hans Wallberg

18 PUBLICATIONS 334 CITATIONS

SEE PROFILE



Bertil Samuelsson

Medivir

162 PUBLICATIONS 4,245 CITATIONS

SEE PROFILE



Mats Larhed

Uppsala University

237 PUBLICATIONS 6,288 CITATIONS

SEE PROFILE

HIV-1 Protease Inhibitors with a Transition-State Mimic Comprising a Tertiary Alcohol: Improved Antiviral Activity in Cells[†]

A.K. Mahalingam,[‡] Linda Axelsson,[‡] Jenny K. Ekegren,[‡] Johan Wannberg,[‡] Jacob Kihlström,[‡] Torsten Unge,[§] Hans Wallberg,^{||} Bertil Samuelsson,^{||} Mats Larhed,^{*,‡} and Anders Hallberg[‡]

[‡]Department of Medicinal Chemistry, Organic Pharmaceutical Chemistry, BMC, Uppsala University, Box 574, SE-751 23 Uppsala, Sweden,

[§]Department of Cell and Molecular Biology, Structural Biology, BMC, Uppsala University, Box 596, SE-751 24 Uppsala, Sweden, and

^{||}Medivir AB, P.O. Box 1086, SE-141 44, Huddinge, Sweden

Received August 5, 2009

By a small modification in the core structure of the previously reported series of HIV-1 protease inhibitors that encompasses a tertiary alcohol as part of the transition-state mimicking scaffold, up to 56 times more potent compounds were obtained exhibiting EC₅₀ values down to 3 nM. Three of the inhibitors also displayed excellent activity against selected resistant isolates of HIV-1. The synthesis of 25 new and optically pure HIV-1 protease inhibitors is reported, along with methods for elongation of the inhibitor P1' side chain using microwave-accelerated, palladium-catalyzed cross-coupling reactions, the biological evaluation, and X-ray data obtained from one of the most potent analogues cocrystallized with both the wild type and the L63P, V82T, I84 V mutant of the HIV-1 protease.

Introduction

Almost three decades after the discovery of AIDS, the pandemic is more severe than ever.¹ There are, however, glimpses of light in this otherwise dark period. The HIV-1 protease inhibitors, introduced in 1995, are certainly a blessing for HIV/AIDS infected patients.^{2–4} In combination with other anti-HIV-1 drugs, the protease inhibitors provide prolonged lifetime and better quality of life by efficiently suppressing the formation of new infectious virus particles in patients. However, two main factors restrict the clinical benefits of this class of antiviral agents. First, many of the HIV-1 protease inhibitors on the market, especially in the first generation, suffer from poor pharmacokinetic properties due to poor aqueous solubility, low metabolic stability, high protein binding, and poor membrane permeability. Because of the pharmacokinetic problems, high doses of drugs are needed in order to keep viral plasma levels down. Poor patient compliance is commonly observed as a consequence of the severe side effects that the high doses give.^{3,5} The new contributions to the available arsenal of HIV-1 protease inhibitors, and the addition of low-dose ritonavir as a pharmacokinetic booster have dealt with many of the pharmacokinetic problems, but there is still room for improvement.^{6–9} Second, the rate at which the virus reproduces and the high number of errors made in the viral replication process create a large amount of mutated viral strains. Thus, resistance toward the marketed HIV-1 protease inhibitors is a serious threat to efficient HIV-treatment.^{6,8,10–14} The development of new HIV-1 protease inhibitors addressing these issues is therefore of high importance.

[†]PDB codes for structure **11** with wild type HIV-1 protease and with mutant strain L63P, V82T, I84 V are 2wkz and 2wl0, respectively.

*To whom correspondence should be addressed. Phone: +46-18-4714667. Fax: +46-18-4714474. E-mail: Mats.Larhed@orgfarm.uu.se.

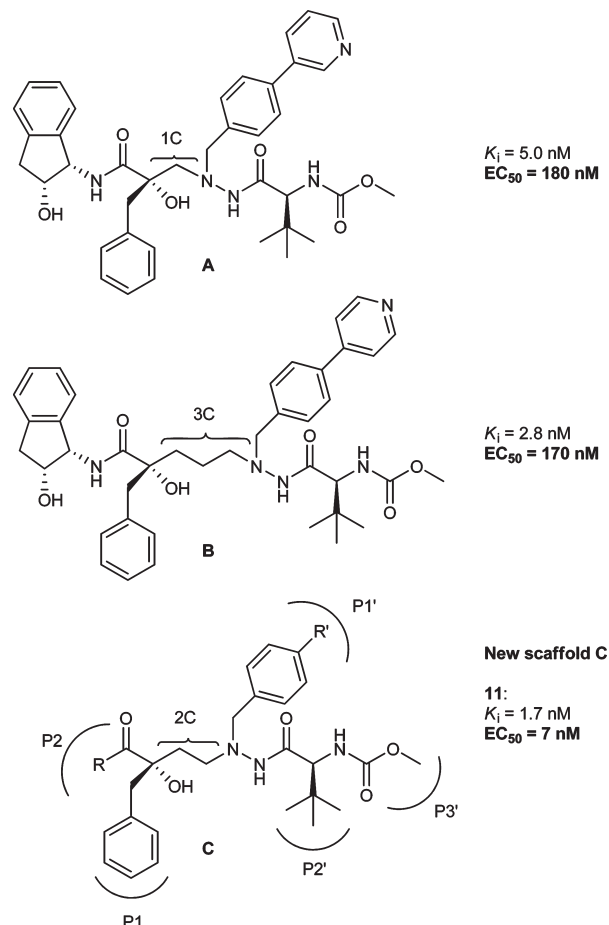
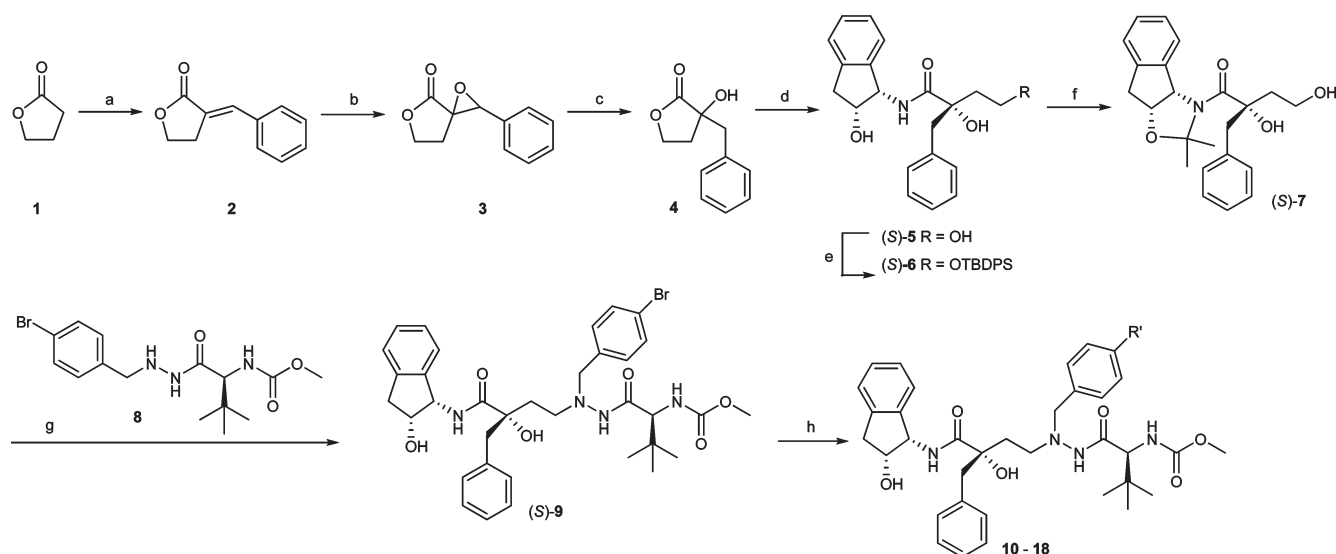


Figure 1. Biological data for compounds **A** and **B** and the general structure of the new series of inhibitors with a shielded hydroxyl group, **C**.

Scheme 1. Synthesis of Inhibitors 10–18^a

^a Reagents and conditions: (a) (1) benzaldehyde, KOtBu, benzene, room temp, (2) H₂SO₄, 56%; (b) *m*CPBA, AIBN, DCE, reflux, 60%; (c) Pd/C, HCOOH, Et₃N, EtOAc, 80 °C, 96%; (d) (1*S*,2*R*)-1-amino-2-indanol, 2-hydroxypyridine, DCM, sealed tube, 60 °C, 66%; (e) TBDPSCl, imidazole, DCM, room temp, 80%; (f) (1) 2-methoxypropene, pyridinium *p*-toluenesulphonic acid, DCM, 0 °C, (2) TBAF, THF, room temp, 69%; (g) (1) Dess–Martin periodinane, DCM, room temp, (2) **8**, Na(OAc)₃BH, AcOH, THF, room temp, 40%; (h) **11**, **12**: R'¹Sn(*n*Bu)₃, Pd(PPh₃)₂Cl₂, CuO, DMF, MW, 120 °C, 50 min, 40% and 31%; **10**, **13–18**: R'-boronic acid/ester, Pd(PPh₃)₂Cl₂, Na₂CO₃ (aq), EtOH, DME, MW, 120 °C, 30 min, 20–62%.

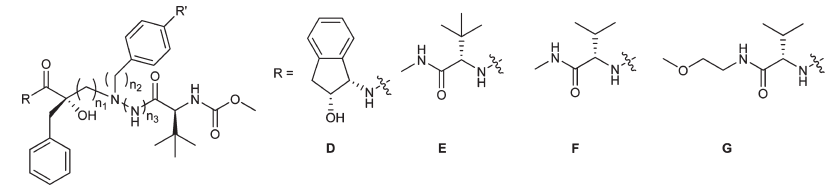
In 2005, we introduced a new class of HIV-1 protease inhibitors, structurally related to indinavir and atazanavir, comprising a shielded tertiary alcohol as part of the transition-state mimicking scaffold, as exemplified by compounds **A**^{15–17} and **B**¹⁸ in Figure 1. A tertiary alcohol unit in the transition-state mimic in protease inhibitors had previously been only briefly reported in the literature, and generally, it resulted in less potent compounds compared to the secondary alcohol analogues.^{19–23} The two reported series of HIV-1 protease inhibitors (Figure 1), both encompassing a tertiary alcohol, differ in the length of the central carbon tether. Potent inhibitors were obtained with *K*_i values down to 2.1 nM, and several of the compounds exhibited excellent membrane permeability in a Caco-2 assay.^{15,16,18} Unfortunately, the compounds had only moderate cellular antiviral activities, the best EC₅₀ value was 170 nM. Furthermore, rapid metabolism of several inhibitors in liver microsomes was encountered, **A** had an intrinsic clearance of 154 μL/min/mg. Although knowing that it is difficult to predict pharmacokinetic outcomes of minor structural modifications, we decided to address an alternative central scaffold of the inhibitors. Thus, we became interested in synthesizing a third series of compounds (**C**, Figure 1), having a two-carbon tether rather than one- and three-carbon tethers (**A** and **B**, Figure 1) between the quaternary carbon and the hydrazide β-nitrogen in the transition-state mimicking scaffold. X-ray structures of the **A** and **B** type of inhibitors combined with computational modeling led us to believe that the hydroxy functionality of the new **C**-class of inhibitors would be positioned closer to Asp-25, possibly increasing potency compared to the previously synthesized inhibitors. Optimization by P1' elongation was performed in order to improve cell-based antiviral activities. Furthermore, the indanolamine moiety present in most of the previously synthesized inhibitors is known to undergo 3'-hydroxylation of the indan and to be metabolically unstable.^{24,25} Therefore a few examples of inhibitors with other P2-groups were assessed in the study. Herein, the synthesis of the new inhibitors, the biological evaluation,

and X-ray data obtained from one of the compounds cocrystallized with both the wild type HIV-1 protease and a clinically relevant mutant of the HIV-1 protease are presented.

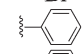
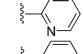
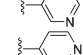
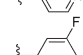
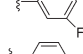
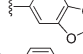
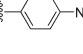
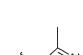
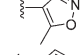
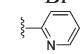
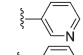
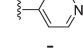
Results

Chemistry. The bromide (*S*)-**9**, serving as an aryl palladium precursor for cross-coupling reactions, was synthesized from commercially available γ-butyrolactone (**1**, Scheme 1). A mixed aldol condensation between this lactone and benzaldehyde gave alkene **2**. *m*CPBA^a epoxidation and palladium(0)-catalyzed reduction resulted in the racemic tertiary alcohol-containing compound **4**. Ring-opening of the lactone moiety by (1*S*,2*R*)-1-amino-2-indanol in the presence of a stoichiometric amount of 2-hydroxypyridine afforded triols (*S*)-**5** and (*R*)-**5**, which were separated by flash column chromatography. Protecting group manipulations were necessary to enable selective oxidation of the primary alcohol in (*S*)-**5**. This was performed via protection of the primary hydroxyl group in (*S*)-**5** with TBDPSCl, subsequent blocking of the secondary alcohol with 2-methoxypropene, followed by deprotection of the TBDPS-group to give (*S*)-**7**. Diol (*S*)-**7** was then oxidized to the corresponding aldehyde using Dess–Martin periodinane. Reductive amination with hydrazide **8**,¹⁵ under acidic conditions, yielded the 4-bromo-substituted inhibitor (*S*)-**9**. The procedure was repeated with (*R*)-**5**, producing diastereomer (*R*)-**9**, which also was evaluated in the enzyme assays. Compound (*S*)-**9** was next used in microwave-accelerated, palladium(0)-catalyzed cross-coupling reactions^{26–30} to afford various para P1'-extended inhibitors, all with retained (*S*)-configuration at the quaternary carbon (Table 1). Stille-couplings were utilized to

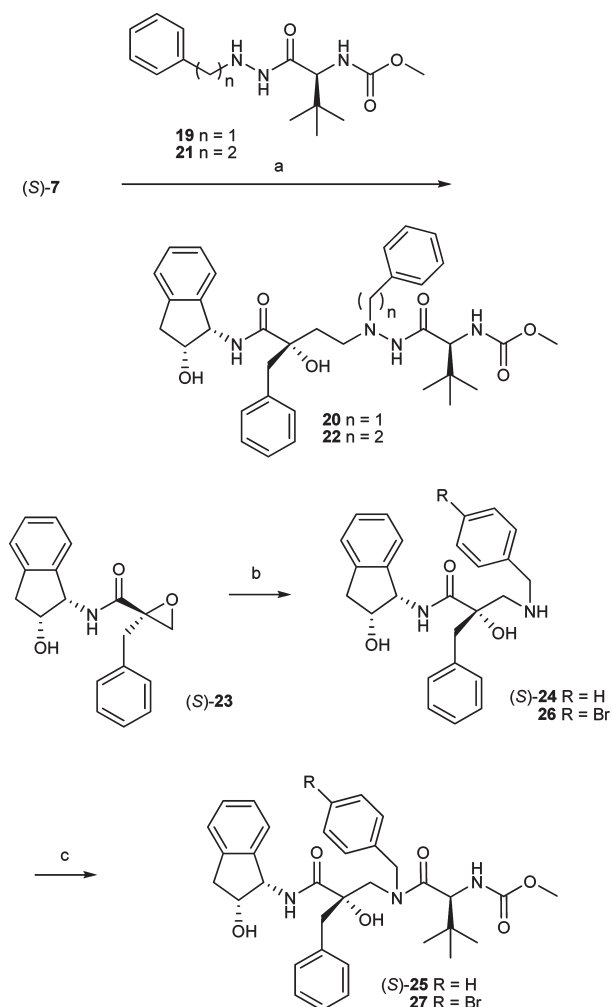
^a Abbreviations: *m*CPBA, 3-chloroperoxybenzoic acid; TBDPSCl, *tert*-butyldiphenylsilylchloride; KOtBu, potassium *tert*-butoxide; AIBN, 2,2'-azobis(2-methylpropionitrile); DCE, 1,2-dichloroethane; TBAF, tetrabutylammonium fluoride; HATU, *N,N,N',N'*-tetramethyl-*O*-(7-azabenzotriazol-1-yl)uronium hexafluorophosphate; DIEA, diisopropylethylamine; IBX, 2-iodoxybenzoic acid; SQV, Saquinavir; RTV, Ritonavir; IDV, Indinavir; LPV, Lopinavir; ATV, Atazanavir; DRV, Darunavir.

Table 1. Synthesis, Enzyme Inhibition Data, Antiviral Activity, and Cytotoxicity of Compounds **9–18**, **20**, **22**, **25**, **27**, and **29–34**^a


The chemical structures for the R, D, E, F, and G groups are shown above the table. R is a general structure with a benzyl group, a hydroxyl group, and a carbamate group. D, E, F, and G are specific structures for the R group, each with different side chains.

Cmpd	Yield (%)	R-group	R'-group	n ₁	n ₂	n ₃	K _i ^b (nM)	EC ₅₀ ^c (nM)	CC ₅₀ (μM)	Cl _{int} (μL/min/mg)	P _{app} ^d (10 ⁻⁶ cm/s)
A	-	D	-	1	1	1	5.0	180	> 10	154	33
B	-	D	-	3	1	1	2.8	170	> 10	94 ^e	3-20
9 ^f	40	D	-Br	2	1	1	2.9	40	7.9	> 300	42
(<i>R</i>)- 9 ^g	36	D	-Br	2	1	1	> 5000	> 10 000	> 10	-	-
10	35	D		2	1	1	12	8	> 10	-	-
11	40	D		2	1	1	1.7	7	> 10	20	3.5
12	31	D		2	1	1	1.2	9	4.9	> 300	26
13	35	D		2	1	1	2.3	3	> 10	-	-
14	50	D		2	1	1	11	13	> 10	-	-
15	62	D		2	1	1	8.0	3	6.1	-	-
16	62	D		2	1	1	1.8	30	> 10	-	-
17	20	D		2	1	1	2.8	5	> 10	-	-
18	51	D		2	1	1	1.7	10	> 10	-	-
20	21	D	-H	2	1	1	2.3	190	> 10	-	-
22	28	D	-H	2	2	1	8.2	6800	> 10	-	-
25	10	D	-H	1	1	0	> 5000	> 10 000	-	-	-
(<i>R</i>)- 25	17	D	-H	1	1	0	> 5000	> 10 000	-	-	-
27	17	D	-Br	1	1	0	> 5000	> 10 000	-	-	-
29	28	E	-Br	2	1	1	1.7	72	> 10	-	-
(<i>R</i>)- 29	26	E	-Br	2	1	1	2200	> 10 000	> 10	-	-
30	3	F	-Br	2	1	1	2.9	160	> 10	-	-
(<i>R</i>)- 30	5	F	-Br	2	1	1	1240	> 10 000	> 10	-	-
31	2	G	-Br	2	1	1	3.2	170	> 10	-	-
(<i>R</i>)- 31	7	G	-Br	2	1	1	2755	> 10 000	> 10	-	-
32	17	E		2	1	1	1.1	47	> 10	-	-
33	44	E		2	1	1	1.0	37	> 10	-	-
34	10	E		2	1	1	2.0	40	> 10	-	-
SQV	-	-	-	-	-	-	0.2 (1.4 ³²)	10 (13 ³²)	-	-	-
RTV	-	-	-	-	-	-	0.8 (4.2 ³²)	50 (70 ³²)	-	-	-
IDV	-	-	-	-	-	-	0.3 (0.5 ³³)	50 (41 ^{3,34})	-	-	-
LPV	-	-	-	-	-	-	1.4 (0.0013 ³⁵)	10 (17 ³⁵)	-	-	-
ATV	-	-	-	-	-	-	0.5 (2.7 ³²)	8 (3.9 ³²)	-	-	-
DRV	-	-	-	-	-	-	1.1 (0.016 ³⁶)	4 (3.7 ³⁷)	-	-	-

^a Reaction conditions: see Schemes 1–3. All the inhibitors have the (*S*) absolute configuration at the tertiary alcohol unless otherwise stated. ^b The K_i values for the marketed drugs are from an in house assay. Values in parentheses are literature data. ^c The EC₅₀ values for the marketed drugs are from an in house assay. Values in parentheses are literature data. ^d Caco-2. ^e Parent compound remaining (%) (PCR). ^f From (*S*)-7. ^g From (*R*)-7.

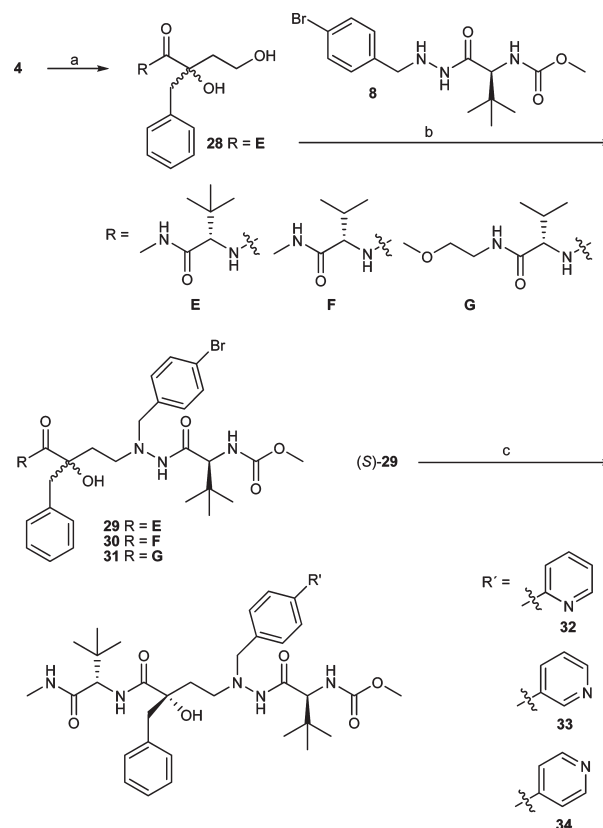
Scheme 2. Synthesis of Inhibitors **20**, **22**, **25**, and **27**^a

^a Reagents and conditions: (a) (1) Dess–Martin periodinane, DCM, room temp, (2) **19** or **21**, Na(OAc)₃BH, AcOH, THF, room temp, 21% and 28%, respectively; (b) benzylamine or 4-bromobenzylamine, Ti(OiPr)₄, dry THF, 34–57%; (c) (S)-2-(methoxycarbonylamino)-3,3-dimethylbutanoic acid, HATU, dry DMF, DIEA, 10–17%. (S)-**25** and **27** were isolated as epimeric mixtures 3:1.

produce pyridines **11** and **12** from the corresponding tributyltin reagents in the microwave cavity. The products **11** and **12** were isolated after purification of the reaction mixtures by preparative RPLC-MS (40% and 31% yield, respectively, Table 1). Compounds **10** and **13–18** were synthesized using Suzuki cross-couplings with boronic acid or ester reactants at 120 °C for 30 min of microwave heating followed by RPLC-MS purification (20–62% yield, Table 1).

Similarly, the P1'-benzyl analogue of (S)-**9**, compound **20**, was synthesized from (S)-**7** and hydrazide **19**¹⁵ (Scheme 2), and derivative **22**, with a one-carbon-elongated P1' group, was produced from hydrazide **21**.³¹ Compounds **25** and **27**, comprising a central amide functionality instead of a hydrazide moiety, making the backbone shorter than for previously synthesized type **A** compounds, were produced by ring-opening of epoxide **23**¹⁵ with benzylamine and 4-bromobenzylamine, followed by amide coupling with (S)-2-(methoxycarbonylamino)-3,3-dimethylbutanoic acid (Scheme 2).

Inhibitors **29–31**, with variation in the P2-position, were synthesized by opening of lactone **4** with (S)-2-amino-N,3,3-trimethylbutanamide (**E**, Scheme 3), affording **28**,

Scheme 3. Synthesis of Inhibitors **29–34**^a

^a Reagents and conditions: (a) (S)-2-amino-N,3,3-trimethylbutanamide or (S)-2-amino-N,3-dimethylbutanamide or (S)-2-amino-N-(2-methoxyethyl)-3-methylbutanamide, 2-hydroxypyridine, DCE, 80 °C, 63–75%; (b) (1) IBX, DCE, 80 °C, (2) **8**, DCE, AcOH, Na(OAc)₃BH, room temp, 2–28%; (c) **32**: 2-pyridylSn(*n*Bu)₃, Pd(PPh₃)₂Cl₂, CuO, DMF, 120 °C, 50 min, 17%. **33**, **34**: R'-B(OH)₂, Pd(OAc)₂, [(*t*-Bu)₃-PH]BF₄, K₂CO₃, H₂O, 1,2-dimethoxyethane, MW, 80 °C, 20 min, 44% and 10%, respectively.

(S)-2-amino-N,3-dimethylbutanamide (**F**, Scheme 3), and (S)-2-amino-N-(2-methoxyethyl)-3-methylbutanamide (**G**, Scheme 3). Only intermediate **28** (R = **E**) was isolated as the primary alcohol and the diastereoisomers separated. In the cases of **30** and **31**, separation of the two diastereoisomers was done after the reductive amination with **8**. P1' variations were again introduced using Suzuki and Stille-cross couplings on (S)-**29** to furnish **32–34**.

Biological Evaluations. Enzyme inhibition data and antiviral activities of compounds **9–18**, **20**, **22**, **25**, **27**, and **29–34** are summarized as *K_i* and EC₅₀ values in Table 1. Previously synthesized derivatives **A** and **B** (Figure 1) are included in Table 1 as reference inhibitors. Compounds **9–18**, **20**, and **22** (excluding (R)-**9**) were potent enzyme inhibitors, with *K_i* values ranging from 1.2 to 12 nM (Table 1). In the cell-based assay, a pronounced P1'-substituent dependence was encountered. The 4-aryl-elongated compounds, except the *p*-amide **16**, displayed excellent antiviral activity, with EC₅₀ values ranging from 3 to 13 nM. The *p*-bromo and unsubstituted benzyl analogues (S)-**9**, **20**, and **22** were less potent and, surprisingly, the one-carbon-elongated derivative **22** was almost inactive in this assay (EC₅₀ = 6800 nM, Table 1). Compounds **25** and **27**, shortened by exchanging the hydrazide core structure with an amide, were also inactive. The P2-varied inhibitors **29–34** showed good protease inhibitory

and antiviral activity, with K_i values from 1.0 to 3.2 nM and EC_{50} values from 37 to 170 nM (Table 1). The (*S*)-configuration of the carbon with the tertiary alcohol was assigned by comparing the potency between inhibitors **29–34** and the inhibitors with indanolamine in the P2-position and was not proven by X-ray crystallography. A rough idea of the inhibitor cytotoxicity is given by the CC_{50} value, which is the inhibitor concentration causing a 50% decrease in cell proliferation. Three of the evaluated compounds displayed cell toxic properties, with CC_{50} values below 10 μ M, including the bromo-, 3-pyridyl, and benzodioxolane derivatives (*S*)-**9**, **12**, and **15** (Table 1). On the basis of the favorable $K_i/EC_{50}/CC_{50}$ profile inhibitor **11**, together with parent inhibitor **9** and related inhibitor **12**, were selected for further studies. The choice of investigating **12** in these assays instead of **13**, with a lower EC_{50} value, was based on the better solubility of nonsymmetric pyridine derivatives. In a liver microsome homogenate, compounds (*S*)-**9** and **12** were extensively degraded by metabolic enzymes and intrinsic clearance values above 300 μ L/min/mg were encountered (Table 1). On the other hand, the 2-pyridyl derivative **11**, with the

Atazanavir prime side, turned out to be considerably more stable, with $Cl_{int} = 20 \mu$ L/min/mg. Compounds (*S*)-**9** and **12** had excellent membrane permeability in a Caco-2 assay (P_{app} (Caco-2) 42×10^{-6} cm/s and 26×10^{-6} cm/s), whereas **11** penetrated more slowly (P_{app} (Caco-2) = 3.5×10^{-6} cm/s).

Inhibitors (*S*)-**9**, **11**, and **12** were further evaluated against selected protease inhibitor resistant isolates of HIV-1. The resistant isolates were obtained by passing cell-free virus in media containing stepwise increased concentrations of saquinavir (entries 2 and 3, Table 2), a symmetric diol based inhibitor^{38,39} (entry 4, Table 2) and ritonavir (entries 5 and 6, Table 2), all known to induce clinically relevant mutations in the HIV-1 protease genome. All three inhibitors were equipotent or more potent toward the viral isolate with G48V and L90M mutations in the protease, commonly encountered in patients treated with saquinavir,¹² compared to the wild-type enzyme (entry 2, Table 2). The V82A and M46I mutations, located in the S1' sub site and the flap region of the enzyme, respectively, are known to cause resistance toward several of the launched HIV-1 protease inhibitors.^{11,13} Interestingly, very high potencies against one of the isolates containing these mutations were obtained with compounds (*S*)-**9**, **11** and **12**, with **11** being equally potent toward this isolate as to the wild-type (entry 4, Table 2). Four mutations, at amino acid 33, 82, 84, and 90, are named universal protease associated mutations (UPAMs) and are very commonly seen in patients failing HIV-therapy.¹² Compounds (*S*)-**9**, **11**, and **12** remain relatively potent when only one UPAM is present (Entries 2, 4, and 5, Table 2), and with two UPAMs, L90 M and I84 V (entry 3, Table 2), but not when both residues 82 and 84 are mutated (entry 6, Table 2).

X-ray Crystallographic Data. The arrangement of compound **11** in the active site of the wild type HIV-1 protease including the most relevant hydrogen bonds, as deduced from the 1.7 Å X-ray structure, with R/R_{free} of 0.23/0.25, (PDB code 2wkz), is illustrated in Figure 2. For comparison,

Table 2. Antiviral Activity Against Selected HIV-1 Protease Inhibitor Resistant Isolates

entry	mutations in protease	EC_{50} (μ M)		
		(<i>S</i>)- 9	11	12
1	wild-type (wt)	0.040	0.007	0.009
2	G48 V, L90M	0.008	0.008	0.010
3	A71 V, I84 V L90M	0.044	0.007	0.019
4	V32I, M46I A71 V, V82A	0.070	0.006	0.014
5	V32I, M46I V82A	0.074	0.024	0.027
6	M46I, V82F, I84 V	0.24	0.13	0.60
		K_i (nM)		
7 ^a	L63P, V82T, I84 V	30	16	16

^a K_i atazanavir 6.5 nM.

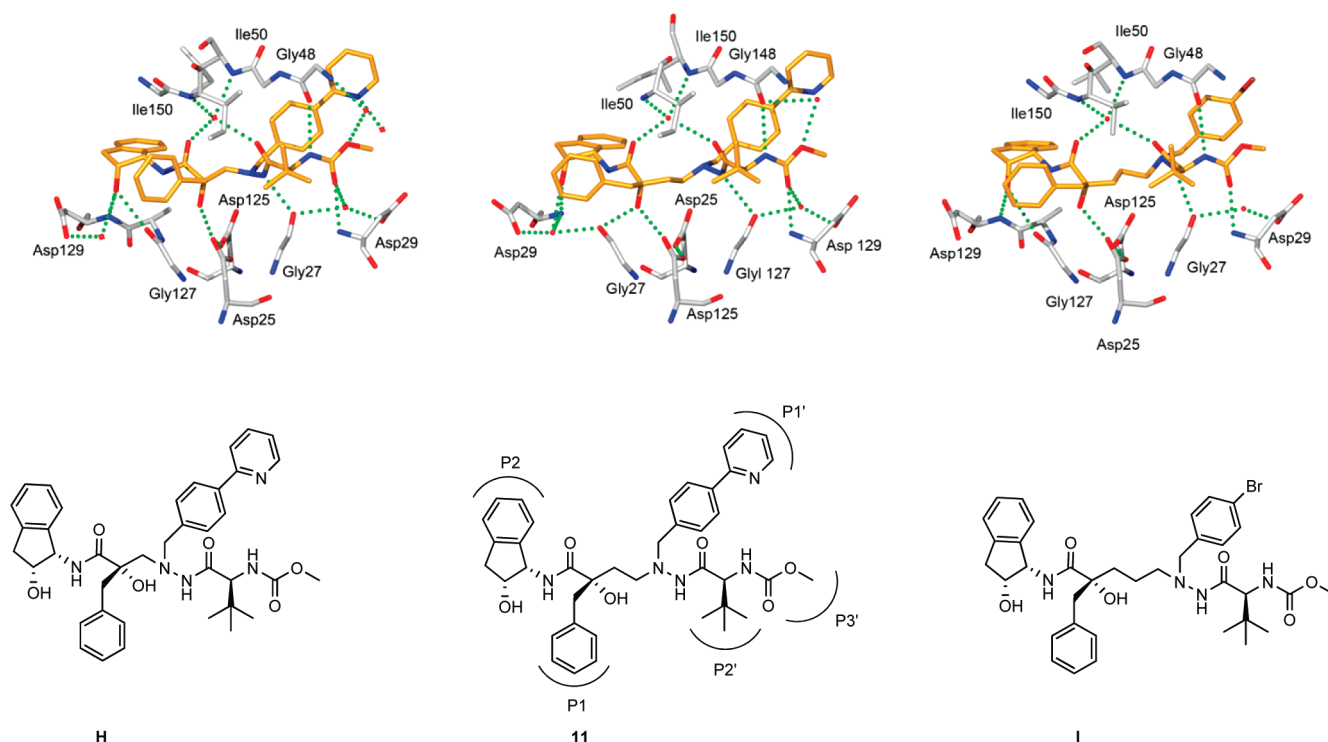


Figure 2. X-ray crystal structures of **H**, **11**, and **I** cocrystallized with HIV-1 protease.

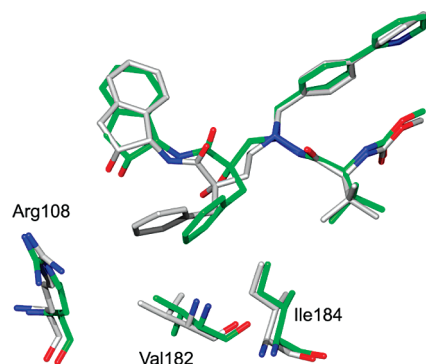


Figure 3. Superimposition of the X-ray structures of inhibitor **11** (gray) and **H** (green).

the previously synthesized **H**¹⁶ with the 1-carbon tether (class **A**) and the 2-pyridyl group in the *para*-benzyl P1' position (PDB code 2cem) and **I**¹⁸ with the 3-carbon tether (class **B**) and the *p*-bromo benzyl side chain in P1' (PDB code 2uxz) are also presented. In the solved structure, compound **11** has rotated 180° in the active site as compared to **H** and **I**. Exemplified by Asp25 from one monomer in the **H/I**-case is assigned as Asp125 from the other monomer in the **11**-case.⁴⁰ The crystal structure of **11** confirmed the (*S*) absolute configuration of the tertiary alcohol. It also showed that while **I** has a distance of 2.9 Å from the tertiary alcohol to Asp25, **11** and **H** both have a shorter binding distance, 2.7 Å to Asp 25/125. Additionally, the tertiary hydroxyl group in **11** has a hydrogen bond to the backbone carbonyl of Gly27 (2.6 Å), while in **H**, the tertiary alcohol is situated too far away (3.3 Å) to form the corresponding hydrogen bond. Compounds **H** and **I** have two hydrogen bonds from the indanolamine hydroxy group to Gly127 and to Asp129, while the same hydroxyl group in **11** has one hydrogen bond to the backbone NH-group of Asp29 (3.0 Å) and one hydrogen bond via a water molecule (3.1 and 2.8 Å). The conserved water molecule that is hydrogen bonded to the nonprime side amide carbonyl, the hydrazide carbonyl, and the enzyme backbone NH-groups of Ile50 and Ile150, arranges similarly in **H**, **11**, and **I**. While structure **11** has seven direct hydrogen bonds to the protein and five bonds via water molecules, inhibitors **H** and **I** have six/five and five/three, respectively.

Superimposition of **H** and **11** reveals a large difference in the location of the P1 benzylic group (Figure 3). The hydrophobic interaction between Val182 and **11** is increased through a change in the position of one of the methyl groups, which bend down toward the benzylic group. The P1 aromatic ring in **11** is close enough to obtain three hydrophobic interactions with one of the methyl groups of Val182.⁴¹ In **H**, only the *para* position of the P1 aromatic ring is close enough to have two hydrophobic interactions with Val82. In this case, the distance is 3.7 Å to one of the methyl groups of Val82 and 3.8 Å to the tertiary carbon. The meta position of the benzylic group in **11** also forms edge on cation- π interactions⁴² with the guanidine amino group of Arg108 (4.0 Å), which are enhanced by the fact that the amino group in Arg108 is tilted toward the inhibitor. The corresponding distance from the benzylic group in **H** to Arg108 is 7.3 Å. On the other hand, **H** is situated closer to Ile84 and has three possible hydrophobic interactions with both the ipso carbon (3.5 Å) and both ortho positions (3.6 and 3.9 Å) of the P1

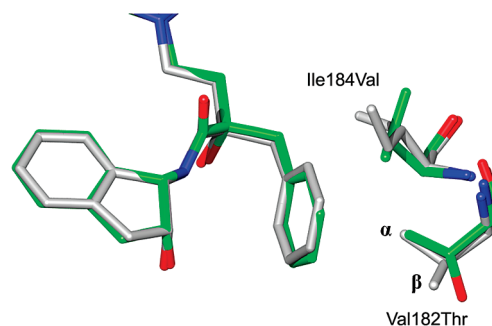


Figure 4. Detail of the superimposition of wt/**11** (shown in gray) and mutant L63P, V82T, I84 V/**11** (shown in green), describing the interaction of the P1-part of inhibitor **11** with V182T and I184 V.

aromatic ring, whereas **11** can only interact with Ile184 via the benzylic carbon (3.4 Å).

The 1.9 Å X-ray structure determination of **11** cocrystallized with the mutant protease L63P, V82T, I84V (PDB code 2wl0), shows a loss of hydrophobic interaction between the benzylic group in P1 and amino acids 182 and 184 after mutating to the less bulky threonine and valine (Figure 4). Both the α - and β -methyl groups of Val182 form hydrophobic interactions with the P1 benzylic moiety,^{41,43} but only the methyl group of the mutant Thr182 forms the corresponding hydrophobic interactions.⁴⁴ There is also an improved hydrophobic interaction between the P1 benzylic carbon and the ethyl group of Ile184 (3.4 Å) compared to the methyl group in the mutated Val184 (4.2 Å). The potency of **11** toward the viral isolate M46I, V82F, I84 V, slightly different from the cocrystallized species, is decreased (entry 6, Table 2). The K_i -value for **11** against L63P, V82T, I84 V is increased 10 times (entry 7, Table 2) compared to the wild type value of 1.7 nM (Table 1).

Discussion

Part of the explanation for the higher inhibiting potency of the type **C** inhibitors with the two-carbon-tether, which is supported by the X-ray crystallography results with inhibitor **11**, is that the tertiary alcohol does not only hydrogen bond to Asp125 but also to the Gly27 carbonyl in the protein backbone. The P1 substituent of **11** also fits much better into the S1 and S3 pockets, as exemplified by the improved interactions with Val182 and Arg108. Importantly, the change of the core scaffold improved the EC₅₀ value from 1100 nM for the *p*-bromo analogue of **A**¹⁶ to 40 nM for (*S*)-**9**. It can be hypothesized that the two-carbon-length scaffold gives this 27-fold improvement in EC₅₀ values due to an improved masking of the tertiary alcohol. Optimization by arylation of the benzylic P1'-part of (*S*)-**9** furnished good cell-based activities, with a 10-fold decrease in EC₅₀ values. A comparison between the results obtained from inhibitor **11** with the corresponding in house assay data for the marketed inhibitors, indinavir and atazanavir, indicates that **11** competes favorably with these drugs. With a K_i value of 1.7 nM, compound **11** is only a few times less potent as atazanavir (K_i = 0.5 nM) and indinavir (K_i = 0.3 nM). Even more interestingly, in the antiviral cell-based assay **11** (EC₅₀ = 7 nM) was considerably more potent than indinavir (EC₅₀ = 50 nM) and was equally potent as atazanavir (EC₅₀ = 8 nM), which was the first protease inhibitor to be given on a once a day basis.⁴⁵ The EC₅₀ value of **11** is also in the same range as lopinavir (EC₅₀ = 10 nM). Compared to the most recent

HIV-1 protease inhibitor on the market, darunavir, **11** is only two times less potent in cell assays than darunavir ($EC_{50} = 4$ nM). HIV-1 protease inhibitors are well-known to be rapidly degraded by cytochrome P-450 enzymes, contributing to a low oral bioavailability of the drugs.⁷ In this sense, inhibitor **11** delivered a favorable result with a reasonably low intrinsic clearance of $20 \mu\text{L}/\text{min}/\text{mg}$ in liver microsomes. The inhibitors where the indanolamine had been replaced with *N*-alkylated amino acid based P2's were less potent, but the known metabolic problems with the indanolamine warrant future investigations. The P_{app} (Caco-2)-values and antiviral activities in the cell assay give somewhat contradictory results, suggesting that the membranes are different in Caco-2 and in HIV-infected MT4 cells (or indicate an activity of membrane transport proteins). Compound **11** has an excellent profile in enzyme assays with HIV-1 protease resistant viral isolates, with the exception of the combined mutations at residues 82 and 84. The reason for that, as can be seen from the cocrystallized X-ray structures, is probably a loss of hydrophobic interactions. Taking all the above-mentioned features into account, inhibitor **11** is a highly promising new lead structure in the development of novel HIV-1 protease inhibitors.

Conclusion

In summary, by modifying the core structure of a series of tertiary alcohol containing HIV-1 protease inhibitors, and by varying the P1' side chains of the structure, as well as the P2 part, compounds exhibiting excellent antiviral activities were obtained (EC_{50} values down to 3 nM). One of the best inhibitors within the series of 25 compounds, **11**, was also potent toward several resistant isolates of HIV-1 and was only slowly degraded by metabolic enzymes. In addition, no signs of cytotoxicity were recorded for this inhibitor. X-ray crystallography data showed a better fit of the P1 moiety of **11** in the S1 and S3 pockets. Also an additional hydrogen bond between the tertiary alcohol in **11** and the HIV-1 protease enzyme was detected, which could explain the higher potencies compared to the previous series.

Experimental Section

General Information. Chemistry. The microwave reactions were performed in a Smith synthesizer producing controlled irradiation at 2450 MHz with a power of 0–300 W. The reaction temperature was determined using the built-in online IR-sensor. Flash column chromatography was performed on Merck silica gel 60 (40–63 μm). Analytical thin layer chromatography was done using aluminum sheets precoated with silica gel 60 F₂₅₄. UV light visualized components. Analytical RPLC-MS was performed on a Gilson HPLC system with a Finnigan AQA quadrupole mass spectrometer with detection by UV (DAD) using an Onyx Monolithic C18 column (50 mm \times 4.6 mm) or a Gilson HPLC system with a Finnigan Thermoquest MSQ quadrupole mass spectrometer with detection by a SEDERE ELSD (Sedex 55) and MS (ESI⁺) using an Onyx Monolithic C18 column (50 mm \times 4.6 mm). For both systems with CH₃CN in 0.05% aqueous HCOOH as mobile phase at a flow rate of 4 mL/min. Preparative RPLC-MS was performed on a Gilson HPLC system with a Finnigan AQA quadrupole mass spectrometer using a Zorbax SB-C8, 5 μm 21.2 mm \times 150 mm (Agilent Technologies) column, with CH₃CN in 0.05% aqueous HCOOH as mobile phase at a flow rate of 15 mL/min. The IMAC support used for metal ion removal was Chelating Superose (32 $\mu\text{mol}/\text{mL}$ Zn²⁺ capacity) prepacked in a 1.5 cm \times 1 cm I.D. column. ¹H and ¹³C NMR spectra were recorded on Varian Mercury

Plus instruments; ¹H at 399.9 MHz and ¹³C at 100.6 MHz or ¹H at 399.8 MHz and ¹³C at 100.5 MHz. 3-[1-Phenyl-meth-(*E*)-ylidene]-dihydro-furan-2-one (**2**),^{46–48} 2-phenyl-1,5-dioxaspiro[2.4]heptan-4-one (**3**),^{48,49} and 3-benzyl-3-hydroxy-dihydro-furan-2-one (**4**)^{46,50} were previously reported. All products were > 95% pure according to LC-MS (ELSD).

Materials. All the reagents were purchased from commercial suppliers and used without further purification. Dichloromethane (DCM) and tetrahydrofuran (THF) were distilled under nitrogen immediately before use. For DCM, calcium hydride was used as a drying agent, and for THF, sodium/benzophenone ketyl were used.

3-[1-Phenyl-meth-(*E*)-ylidene]-dihydro-furan-2-one (2**).** To a cooled (0 °C) solution of γ -butyrolactone (5.0 g, 58 mmol) and benzaldehyde (5.85 g, 55.1 mmol) in dry benzene (75 mL) was added K⁺OrBu (7.82 g, 69.7 mmol) portionwise. After the addition, the thick orange solution was stirred at room temp for 6 h. The mixture was acidified with dilute H₂SO₄ (aq) and extracted with Et₂O (3 \times 30 mL). The organic layer was dried (MgSO₄) and evaporated under reduced pressure. The residue was purified on flash column chromatography (silica gel, EtOAc/petroleum ether, 1:5) to yield **2** (5.4 g, 56%) as a white solid. ¹H NMR (CDCl₃, 400 MHz): δ 7.94 (s, 1H), 7.49–7.34 (m, 5H), 3.91 (m, 2H), 2.85 (m, 2H). ¹³C NMR (CDCl₃, 100 MHz): δ 172.8, 136.9, 134.9, 130.3, 130.1, 129.2, 123.8, 65.8, 27.7.

2-Phenyl-1,5-dioxaspiro[2.4]heptan-4-one (3**).** To a solution of **2** (4.0 g, 22.9 mmol) and 3-chloroperoxybenzoic acid (6.18 g, 27.6 mmol) in DCE (70 mL) was added AIBN (50 mg) at 80 °C, and the mixture was refluxed in the dark for 6 h. The resulting solution was cooled and filtered, the solvent was removed under reduced pressure, and the residue dissolved in DCM. The organic phase was washed successively with saturated, aqueous solutions of NaHCO₃ (20 mL), KI (20 mL), Na₂S₂O₃ (20 mL), and NaHCO₃ (20 mL) and then dried (MgSO₄) and evaporated under reduced pressure. Purification by flash column chromatography (silica gel, EtOAc/petroleum ether, 1:4) gave **3** (2.62 g, 60%) as a white solid. A similar reaction without AIBN gave **3** in 46% yield. The material had spectroscopic properties identical with those reported in the literature.⁴⁹

3-Benzyl-3-hydroxy-dihydro-furan-2-one (4**).** To a mixture of **3** (1.90 g, 10 mmol), Pd/C (Degussa type E101 NE/W, 0.53 g, 2.5 mol % Pd), and 20 mL of EtOAc in a reaction tube was added formic acid (604 μL , 16 mmol) and triethylamine (2.09 mL, 15 mmol). The tube was sealed with a screw cap and heated at 80 °C for 3 h. The reaction mixture was allowed to cool to room temperature, the catalyst was filtered off, and volatiles were evaporated under reduced pressure. The residue was purified by silica flash column chromatography (*i*-hexane/EtOAc 1:1) to give the alcohol as a colorless solid (1.85 g, 9.63 mmol, 96%). ¹H NMR (CDCl₃, 400 MHz): δ 7.34–7.23 (m, 5H), 4.26 (m, 1H), 3.75 (m, 1H), 3.05 (s, 2H), 3.04 (s, 1H), 2.39–2.24 (m, 2H). ¹³C NMR (CDCl₃, 100 MHz): δ 178.9, 134.2, 130.1, 128.7, 127.5, 75.5, 65.3, 43.4, 34.0.

(*S*)-2-Benzyl-2,4-dihydroxy-*N*-((1*S*,2*R*)-2-hydroxy-indan-1-yl)-butyramide ((*S*)-5**).** To compound **4** (0.5 g, 2.6 mmol) and 2-hydroxypyridine (0.27 g, 2.8 mmol) in dry DCM (15 mL) was added (1*S*,2*R*)-1-amino-2-indanol (0.43 g, 2.8 mmol). The reaction mixture was stirred at 60 °C for 24 h in a sealed tube and then evaporated. The residue was dissolved in EtOAc (80 mL) and washed with 1 M HCl (20 mL), followed by saturated aqueous NaHCO₃ (20 mL) and thereafter dried (MgSO₄), filtered, and evaporated. The residue was purified by flash column chromatography (silica gel, acetone/petroleum ether, 1:3) yielding the two diastereomeric triols; (*S*)-**5** (0.26 g) and (*R*)-**5** (0.33 g) as white solids in a total yield of 66%. ¹H NMR (CD₃OD, 400 MHz): δ 7.29–7.15 (m, 9H), 5.11 (d, *J* = 4.8 Hz, 1H), 4.19 (m, 1H), 3.82 (m, 2H), 3.13–3.05 (m, 2H), 2.96–2.80 (m, 2H), 2.30 (m, 1H), 1.93 (m, 1H). ¹³C NMR (CD₃OD, 100 MHz): δ 176.1, 141.3, 140.3, 136.5, 130.4, 127.7, 127.6, 126.6, 126.4, 125.0, 124.0, 78.3, 72.7, 58.4, 57.1, 45.7, 40.3, 39.7.

(S)-2-Benzyl-4-(tert-butyl-diphenyl-silanyloxy)-2-hydroxy-N-((1S,2R)-2-hydroxy-indan-1-yl)-butyramide ((S)-6). To a stirred solution of (S)-5 (0.245 g, 0.72 mmol) and imidazole (0.073 g, 1.08 mmol) in dry DCM (25 mL) was added TBDPS-Cl (0.2 g, 0.75 mmol) and left overnight with stirring. The reaction mixture was diluted, washed with water, dried (MgSO₄), evaporated, and purified by flash column chromatography to yield (S)-6 (0.334 g, 80%). ¹H NMR (CDCl₃, 400 MHz): δ 7.71–7.66 (m, 4H), 7.48–7.36 (m, 8H), 7.34–7.24 (m, 4H), 7.22–7.18 (m, 2H), 7.12–7.04 (m, 2H), 5.37 (s, 1H), 5.24 (m, 1H), 4.16–3.95 (m, 3H), 3.10 (d, *J* = 13.6 Hz, 1H), 3.05 (m, 2H), 2.81 (d, *J* = 16.4 Hz, 1H), 2.40 (m, 1H), 2.15 (m, 1H), 1.09 (s, 9H). ¹³C NMR (CDCl₃, 100 MHz): δ 174.8, 140.7, 137.1, 135.7, 135.6, 132.3, 131.0, 130.4, 128.3, 128.2, 128.1, 127.1, 127.0, 125.3, 124.0, 80.9, 73.4, 63.3, 57.4, 46.4, 39.1, 38.9, 27.9, 19.2.

(S)-2-Benzyl-1-((3aS,8aR)-2,2-dimethyl-8,8a-dihydro-3aH-indeno[1,2-d]oxazol-3-yl)-2,4-dihydroxy-butan-1-one ((S)-7). To a cooled (0 °C) solution of (S)-6 (0.325 g, 0.56 mmol) and pyridinium *p*-toluenesulphonic acid (15 mg, 0.05 mmol) in dry DCM (20 mL), 2-methoxypropene (0.4 g, 5.6 mmol) was added and stirred for 6 h at the same temperature. The solution was washed with saturated NaHCO₃ (aq) and brine, dried (MgSO₄), and evaporated under reduced pressure. The crude product [0.33 g, MS (ESI⁺): *m/z* 620 (M+H⁺)] was dissolved in THF (20 mL), TBAF (0.278 g, 1.06 mmol, 1 M in THF) was added at room temp, and the mixture was stirred for 3 h. The solvent was evaporated and the residue dissolved in DCM, washed with water and brine, dried (MgSO₄), and evaporated. The product was purified by flash column chromatography (silica gel, acetone/petroleum ether, 1:4) yielding (S)-7 (0.145 g, 69%) as a white solid. ¹H NMR (CDCl₃, 400 MHz): δ 7.34–7.25 (m, 4H), 7.20–7.09 (m, 5H), 5.25 (m, 1H), 4.23 (m, 1H), 4.10–4.00 (m, 2H), 3.15 (d, *J* = 12.8 Hz, 1H), 3.06 (dd, *J* = 5.6, 16.4 Hz, 1H), 2.96 (d, *J* = 13.2 Hz, 1H), 2.83 (d, *J* = 16.8 Hz, 1H), 2.40 (m, 1H), 2.16 (s, 3H), 2.10 (m, 1H), 1.05 (s, 3H). ¹³C NMR (CDCl₃, 100 MHz): δ 175.9, 140.7, 140.5, 136.7, 130.9, 128.3, 127.3, 127.2, 125.4, 124.0, 102.5, 80.3, 73.3, 61.2, 57.6, 46.2, 39.3, 39.2, 31.2, 29.5.

((S)-1-[N'-(4-Bromo-benzyl)-N'-((S)-3-hydroxy-3-((1S,2R)-2-hydroxy-indan-1-ylcarbamoyl)-4-phenyl-butyl)-hydrazinocarbonyl]-2,2-dimethyl-propyl)-carbamic Acid Methyl Ester ((S)-9). A solution of (S)-7 (0.13 g, 0.34 mmol) in dry DCM (5 mL) was added over 1 min to a stirred solution of Dess–Martin periodinane (0.16 g, 0.37 mmol) in dry DCM (10 mL). After 30 min, the homogeneous mixture was diluted with ether and poured into cold saturated NaHCO₃ (aq, 10 mL) containing Na₂S₂O₃ (2.2 g). The organic layer was washed with saturated NaHCO₃ (aq) and brine, dried (MgSO₄), and evaporated below 20 °C to yield the crude aldehyde [0.082 g, MS (ESI⁺): *m/z* 380 (M+H⁺)]. To the aldehyde (0.082 g, 0.21 mmol) and ((S)-1-[N'-(4-bromo-benzyl)-hydrazinocarbonyl]-2,2-dimethyl-propyl)-carbamic acid methyl ester **8** (0.086 g, 0.23 mmol) in dry THF (10 mL) was added acetic acid (0.025 g, 0.42 mmol), and the mixture was stirred for 10 min and then Na(OAc)₃BH (0.133 g, 0.63 mmol) was added and stirring was continued overnight. The reaction mixture was quenched with water and evaporated. The residue was dissolved in DCM (20 mL) and washed with water and brine, and then trifluoroacetic acid (1 mL) was added and the organic layer was stirred for 30 min. The mixture was evaporated and washed successively with saturated NaHCO₃ (aq), water, and brine and dried (MgSO₄). The product was purified on flash column chromatography (silica gel, acetone/petroleum ether, 1:3) to yield (S)-9 (0.58 g, 40%). ¹H NMR (CDCl₃, 400 MHz): δ 7.40–7.09 (m, 13H), 5.07 (d, *J* = 5.2 Hz, 1H), 4.27 (m, 1H), 3.70 (m, 6H), 3.10–2.78 (m, 6H), 2.20 (m, 1H), 1.92 (m, 1H), 0.69 (s, 9H). ¹³C NMR (CD₃OD, 100 MHz): δ 177.8, 172.4, 159.1, 142.6, 141.7, 138.1, 137.7, 132.4, 131.8, 129.1, 128.9, 127.9, 127.6, 126.3, 125.5, 122.4, 79.9, 73.8, 63.2, 62.4, 58.4, 55.3, 52.9, 47.2, 40.9, 35.7, 34.7, 26.9.

{(S)-1-[N'-((S)-3-Hydroxy-3-((1S,2R)-2-hydroxy-indan-1-ylcarbamoyl)-4-phenyl-butyl)-N'-(4-pyridin-2-yl-benzyl)-hydrazinocarbonyl]-2,2-dimethyl-propyl}-carbamic Acid Methyl Ester (11). Pd(PPh₃)₂Cl₂ (4.61 mg, 0.0065 mmol) was added to a solution of (S)-9 (90 mg, 0.129 mmol), 2-(1,1,1-tri-*n*-butylstannyl)pyridine (0.191 g, 0.51 mmol), and CuO (10.3 mg, 0.129 mmol) in DMF (2.0 mL) and stirred in a sealed, heavy-walled Smith process vial at 120 °C for 50 min in the microwave cavity. The mixture was diluted with DCM (25 mL) and washed with saturated NaHCO₃ (aq, 3 × 15 mL). The organic layer was dried (MgSO₄) and evaporated. The residue was redissolved in CH₃CN (60 mL) and washed with isohexane (3 × 20 mL). The acetonitrile phase was evaporated, and the crude product was purified using RPLC-MS (45 min gradient of 15–70% CH₃CN in 0.05% aq formic acid), followed by a passage through an IMAC column in order to remove metal ions, yielding **11** (36.2 mg, 40%) as a white solid. ¹H NMR (CD₃OD 400 MHz): δ 8.56 (m, 1H), 7.82 (m, 1H), 7.72–7.60 (m, 4H), 7.54 (m, 1H), 7.44 (m, 1H), 7.34–7.16 (m, 6H), 7.06–7.00 (m, 3H), 6.96 (m, 1H), 4.96 (m, 1H), 4.16 (m, 1H), 3.82 (m, 2H), 3.70 (m, 1H), 3.60 (s, 3H), 3.08–2.78 (m, 6H), 2.10 (m, 1H), 1.94 (m, 1H), 0.78 (s, 9H). ¹³C NMR (CD₃OD, 100 MHz): δ 176.9, 171.5, 158.2, 157.7, 149.1, 141.5, 140.5, 138.6, 138.1, 138.0, 137.2, 132.9, 132.3, 132.2, 130.8, 129.9, 129.2, 129.1, 127.9, 127.3, 126.9, 126.6, 125.0, 124.5, 122.8, 121.7, 79.3, 73.1, 62.3, 57.7, 53.6, 51.9, 46.6, 39.8, 34.5, 33.9, 26.1.

Acknowledgment. We acknowledge the financial support from the Swedish Research Council (VR), Knut and Alice Wallenberg's Foundation and Medivir AB. We thank Dr. Lotta Vrang and Dr. Åsa Rosenquist for discussions and testing of the mutant isolates. We also thank Mr. Oskar Enström for help with crystal production.

Supporting Information Available: Experimental details and spectroscopic data for compounds **2–7**, **9–18**, **20**, **22**, **24–34**, elemental analysis data, X-ray crystal structures and determination details, procedures for enzyme, antiviral activity and Caco-2 assays, and liver microsome stability evaluation. This material is available free of charge via the Internet at <http://pubs.acs.org>.

References

- (1) Joint United Nations Programme on HIV/AIDS *AIDS Epidemic Update: December 2007*; UNAIDS/WHO: Geneva, **2007**.
- (2) Brik, A.; Wong, C.-H. HIV-1 protease: mechanism and drug discovery. *Org. Biomol. Chem.* **2003**, *1*, 5–14.
- (3) Randolph, J. T.; DeGoey, D. A. Peptidomimetic inhibitors of HIV protease. *Curr. Top. Med. Chem.* **2004**, *4*, 1079–1095.
- (4) Abdel-Rahman, H. M.; Al-Karamany, G. S.; El-Koussi, N. A.; Youssef, A. F.; Kiso, Y. HIV protease inhibitors: peptidomimetic drugs and future perspectives. *Curr. Med. Chem.* **2002**, *9*, 1905–1922.
- (5) Rodríguez-Barrios, F.; Gago, F. HIV protease inhibition: limited recent progress and advances in understanding current pitfalls. *Curr. Top. Med. Chem.* **2004**, *4*, 991–1007.
- (6) Aruksakunwong, O.; Promsri, S.; Wittayanarakul, K.; Nimmanpipug, P.; Lee, V. S.; Wijitkosoom, A.; Sompornpisut, P.; Hannongbua, S. Current development on HIV-1 protease inhibitors. *Curr. Comput.-Aided Drug Des.* **2007**, *3*, 201–213.
- (7) Armbruster, C. HIV-1 infection: recent developments in treatment and current management strategies. *Anti-Infect. Agents Med. Chem.* **2008**, *7*, 201–214.
- (8) Anderson, J.; Schiffer, C.; Lee, S.-K.; Swanstrom, R. Viral protease inhibitors. *Handb. Exp. Pharmacol.* **2009**, *189*, 85–110.
- (9) Mastrolorenzo, A.; Rusconi, S.; Scozzafava, A.; Barbaro, G.; Supuran, C. T. Inhibitors of HIV-1 protease: current state of the art 10 years after their introduction. From antiretroviral drugs to antifungal, antibacterial and antitumor agents based on aspartic protease inhibitors. *Curr. Med. Chem.* **2007**, *14*, 2734–2748.
- (10) Ghosh, A. K.; Sridhar, P. R.; Leshchenko, S.; Hussain, A. K.; Li, J.; Kovalevsky, A. Y.; Walters, D. E.; Wedekind, J. E.

- Grum-Tokars, V.; Das, D.; Koh, Y.; Maeda, K.; Gatanaga, H.; Weber, I. T.; Mitsuya, H. Structure-Based Design of Novel HIV-1 Protease Inhibitors To Combat Drug Resistance. *J. Med. Chem.* **2006**, *49*, 5252–5261.
- (11) Clavel, F.; Hance, A. J. HIV drug resistance. *N. Engl. J. Med.* **2004**, *350*, 1023–1035.
- (12) de Mendoza, C.; Soriano, V. Resistance to HIV protease inhibitors: mechanisms and clinical consequences. *Curr. Drug Metab.* **2004**, *5*, 321–328.
- (13) Menéndez-Arias, L. Targeting HIV: antiretroviral therapy and development of drug resistance. *Trends Pharmacol. Sci.* **2002**, *23*, 381–388.
- (14) Hertogs, K.; Bloor, S.; Kemp, S. D.; Van den Eynde, C.; Alcorn, T. M.; Pauwels, R.; Van Houtte, M.; Staszewski, S.; Miller, V.; Larder, B. A. Phenotypic and genotypic analysis of clinical HIV-1 isolates reveals extensive protease inhibitor cross-resistance: a survey of over 6000 samples. *AIDS (London, England)* **2000**, *14*, 1203–1210.
- (15) Ekegren, J. K.; Unge, T.; Safa, M. Z.; Wallberg, H.; Samuelsson, B.; Hallberg, A. A new class of HIV-1 protease inhibitors containing a tertiary alcohol in the transition-state mimicking scaffold. *J. Med. Chem.* **2005**, *48*, 8098–8102.
- (16) Ekegren, J. K.; Ginman, N.; Johansson, Å.; Wallberg, H.; Larhed, M.; Samuelsson, B.; Unge, T.; Hallberg, A. Microwave accelerated synthesis of P1'-extended HIV-1 protease inhibitors encompassing a tertiary alcohol in the transition-state mimicking scaffold. *J. Med. Chem.* **2006**, *49*, 1828–1832.
- (17) Ekegren, J. K.; Gising, J.; Wallberg, H.; Larhed, M.; Samuelsson, B.; Hallberg, A. Variations of the P2 group in HIV-1 protease inhibitors containing a tertiary alcohol in the transition-state mimicking scaffold. *Org. Biomol. Chem.* **2006**, *4*, 3040–3043.
- (18) Wu, X.; Öhrngren, P.; Ekegren, J. K.; Unge, J.; Unge, T.; Wallberg, H.; Samuelsson, B.; Hallberg, A.; Larhed, M. Two-Carbon-Elongated HIV-1 Protease Inhibitors with a Tertiary-Alcohol-Containing Transition-State Mimic. *J. Med. Chem.* **2008**, *51*, 1053–1057.
- (19) Rich, D. H.; Bernatowicz, M. S.; Agarwal, N. S.; Kawai, M.; Salituro, F. G.; Schmidt, P. G. Inhibition of aspartic proteases by pepstatin and 3-methylstatine derivatives of pepstatin. Evidence for collected-substrate enzyme inhibition. *Biochemistry* **1985**, *24*, 3165–3173.
- (20) Rich, D. H. Pepstatin-derived inhibitors of aspartic proteinases. A close look at an apparent transition-state analog inhibitor. *J. Med. Chem.* **1985**, *28*, 263–273.
- (21) Agarwal, N. S.; Rich, D. H. Inhibition of cathepsin D by substrate analogs containing statine and by analogs of pepstatin. *J. Med. Chem.* **1986**, *29*, 2519–2524.
- (22) Godfrey, J. D., Jr.; Gordon, E. M.; Von Langen, D. J. Synthesis of peptide-derived amino alcohols II. Synthetic methodology for the preparation of tertiary alcohols. *Tetrahedron Lett.* **1987**, *28*, 1603–1606.
- (23) Kim, B. M.; Guare, J. P.; Hanifin, C. M.; Arford-Bickerstaff, D. J.; Vacca, J. P.; Ball, R. G. A convergent synthesis of novel conformationally restricted HIV-1 protease inhibitors. *Tetrahedron Lett.* **1994**, *35*, 5153–5156.
- (24) Balani, S. K.; Arison, B. H.; Mathai, L.; Kauffman, L. R.; Miller, R. R.; Stearns, R. A.; Chen, I. W.; Lin, J. H. Metabolites of L-735,524, a potent HIV-1 protease inhibitor, in human urine. *Drug Metab. Dispos.* **1995**, *23*, 266–270.
- (25) Lin, J. H. Role of pharmacokinetics in the discovery and development of indinavir. *Adv. Drug Delivery Rev.* **1999**, *39*, 33–49.
- (26) Larhed, M.; Moberg, C.; Hallberg, A. Microwave-accelerated homogeneous catalysis in organic chemistry. *Acc. Chem. Res.* **2002**, *35*, 717–727.
- (27) Ersmark, K.; Larhed, M.; Wannberg, J. Microwave-enhanced medicinal chemistry: A high-speed opportunity for convenient preparation of protease inhibitors. *Curr. Opin. Drug Discovery Dev.* **2004**, *7*, 417–427.
- (28) Kappe, C. O.; Dallinger, D. The impact of microwave synthesis on drug discovery. *Nat. Rev. Drug Discovery* **2006**, *5*, 51–63.
- (29) Caddick, S.; Fitzmaurice, R. Microwave enhanced synthesis. *Tetrahedron* **2009**, *65*, 3325–3355.
- (30) Larhed, M.; Hallberg, A. Microwave-Promoted Palladium-Catalyzed Coupling Reactions. *J. Org. Chem.* **1996**, *61*, 9582–9584.
- (31) Hydrazides **19** and **21** were kindly supplied by Dr. Kristina Örrling, Department of Medicinal Chemistry, Uppsala University, Sweden.
- (32) Robinson, B. S.; Riccardi, K. A.; Gong, Y.-F.; Guo, Q.; Stock, D. A.; Blair, W. S.; Terry, B. J.; Deminie, C. A.; Djang, F.; Colonna, R. J.; Lin, P.-F. BMS-232632, a highly potent human immunodeficiency virus protease inhibitor that can be used in combination with other available antiretroviral agents. *Antimicrob. Agents Chemother.* **2000**, *44*, 2093–2099.
- (33) Dorsey, B. D.; Levin, R. B.; McDaniel, S. L.; Vacca, J. P.; Guare, J. P.; Darke, P. L.; Zugay, J. A.; Emini, E. A.; Schleif, W. A.; Quintero, J. C.; Lin, J. H.; Chen, I.-W.; Holloway, M. K.; Fitzgerald, P. M. D.; Axel, M. G.; Ostovic, D.; Anderson, P. S.; Huff, J. R. L-735,524: the design of a potent and orally bioavailable HIV protease inhibitor. *J. Med. Chem.* **1994**, *37*, 3443–3451.
- (34) Molla, A.; Vasavanonda, S.; Kumar, G.; Sham, H. L.; Johnson, M.; Grabowski, B.; Denissen, J. F.; Kohlbrenner, W.; Plattner, J. J.; Leonard, J. M.; Norbeck, D. W.; Kempf, D. J. Human serum attenuates the activity of protease inhibitors toward wild-type and mutant human immunodeficiency virus. *Virology* **1998**, *250*, 255–262.
- (35) Sham, H. L.; Kempf, D. J.; Molla, A.; Marsh, K. C.; Kumar, G. N.; Chen, C. M.; Kati, W.; Stewart, K.; Lal, R.; Hsu, A.; Betebenner, D.; Korneyeva, M.; Vasavanonda, S.; McDonald, E.; Saldivar, A.; Wideburg, N.; Chen, X.; Niu, P.; Park, C.; Jayanti, V.; Grabowski, B.; Granneman, G. R.; Sun, E.; Japour, A. J.; Leonard, J. M.; Plattner, J. J.; Norbeck, D. W. ABT-378, a highly potent inhibitor of the human immunodeficiency virus protease. *Antimicrob. Agents Chemother.* **1998**, *42*, 3218–3224.
- (36) Ghosh Arun, K.; Dawson Zachary, L.; Mitsuya, H. Darunavir, a conceptually new HIV-1 protease inhibitor for the treatment of drug-resistant HIV. *Bioorg. Med. Chem.* **2007**, *15*, 7576–7580.
- (37) De Meyer, S.; Azijn, H.; Surleraux, D.; Jochmans, D.; Tahri, A.; Pauwels, R.; Wigerinck, P.; de Bethune, M.-P. TMC114, a novel human immunodeficiency virus type 1 protease inhibitor active against protease inhibitor-resistant viruses, including a broad range of clinical isolates. *Antimicrob. Agents Chemother.* **2005**, *49*, 2314–2321.
- (38) "N1,N6-Di[(1S)-2-methyl-1-(methylcarbamoyl)propyl]-(2R,3R,4R,5R)-2,5-di(benzyloxy)-3,4-dihydroxyhexanediamide.
- (39) Alterman, M.; Björnsen, M.; Muehlman, A.; Classon, B.; Kvarnström, I.; Danielson, H.; Markgren, P.-O.; Nilroth, U.; Unge, T.; Hallberg, A.; Samuelsson, B. Design and synthesis of new potent C2-symmetric HIV-1 protease inhibitors. Use of L-mannaric acid as a peptidomimetic scaffold. *J. Med. Chem.* **1998**, *41*, 3782–3792.
- (40) Bagossi, P.; Cheng, Y.-S. E.; Oroszlan, S.; Tozser, J. Comparison of the specificity of homo- and heterodimeric linked HIV-1 and HIV-2 proteinase dimers. *Protein Eng.* **1998**, *11*, 439–445.
- (41) The alpha-methyl group of Val 182 (Figure 4) has a distance of 3.8 Å to one of the ortho, 3.8 Å to the meta and 3.9 Å to the para carbon of the inhibitor benzyl group.
- (42) Gallivan, J. P.; Dougherty, D. A. Cation- π interactions in structural biology. *Proc. Natl. Acad. Sci. U.S.A.* **1999**, *96*, 9459–9464.
- (43) The beta-methyl group of Val182 (Figure 4) has a distance of 5.1 Å to the ortho, 4.3 and 4.4 Å to the meta positions, and 3.9 Å to the para position of the inhibitor benzyl group.
- (44) The methyl group of mutant Thr182 (Figure 4) has a distance of 4.0 Å to the ipso, 3.8 Å to the ortho, 3.7 Å to the meta, and 3.8 Å to the para carbon. The distance to the hydroxy oxygen is 5.7 Å for the ortho, 5.1 Å for the meta, and 5.0 Å for the para carbon of the inhibitor benzyl group.
- (45) Wang, F.; Ross, J. Atazanavir: a novel azapeptide inhibitor of HIV-1 protease. *Formulary* **2003**, *38*, 691–702.
- (46) Ekegren, J.; Hallberg, A.; Wallberg, H.; Samuelsson, B.; Mahalingam, K. Preparation of amino acid hydrazide derivatives and related compounds as HIV protease inhibitors. Patent WO 2006084688, **2006**.
- (47) Moiese, J.; Arseniyadis, S.; Cossy, J. Cross-Metathesis between alpha-Methylene-gamma-butyrolactone and Olefins: A Dramatic Additive Effect. *Org. Lett.* **2007**, *9*, 1695–1698.
- (48) Murray, A. W.; Reid, R. G. Convenient synthesis of alpha-epoxylactones (4-oxo-1,5-dioxaspiro[2.4]heptanes and -[2.5]octanes). *Synthesis* **1985**, 35–38.
- (49) Shibata, I.; Yamasaki, H.; Baba, A.; Matsuda, H. A Novel Darzens type reaction promoted by tributylstannylcarbamate. *J. Org. Chem.* **1992**, *57*, 6909–6914.
- (50) Curran, D. P.; Ko, S.-B. Synthesis of Optically Active alpha-Hydroxy Lactones by Sharpless Asymmetric Dihydroxylations of Ketene Acetals, Enol Ethers, and Ene Lactones. *J. Org. Chem.* **1994**, *59*, 6139–6141.